JOC*Article*

Metal-Directed Self-Assembly of Cavitand Frameworks

Edoardo Menozzi,[†] Marco Busi,[†] Chiara Massera,[‡] Franco Ugozzoli,[‡] Daniele Zuccaccia,[§] Alceo Macchioni,[§] and Enrico Dalcanale*[,†]

Dipartimento di Chimica Organica ed Industriale and Unità INSTM, Università di Parma, Parco Area delle Scienze 17/A, 43100 Parma, Italy, Dipartimento di Chimica Generale ed Inorganica, Chimica Analitica, Chimica Fisica, Università di Parma, Parco Area delle Scienze 17/A, 43100 Parma, Italy, and Dipartimento di Chimica, Università di Perugia, Via Elce di Sotto, 8-06123 Perugia, Italy

enrico.dalcanale@unipr.it

Received November 29, 2005

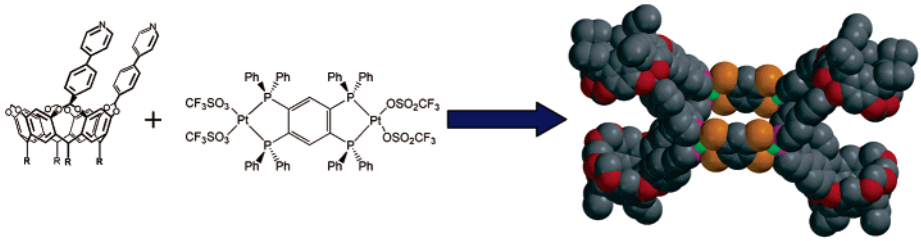

The self-assembly between bidentate cavitand ligands and mono/dinuclear metal precursors to give cavitand frameworks has been explored. For this purpose, two new cavitands bearing *AB* and *AC* phenylpyridyl moieties at the upper rim have been synthesized. A series of self-assembled molecular dimers featuring *fac*-$Re(CO)_3Br$ as metal corners have been prepared and characterized. Two possible dimeric structures (C-shaped and S-shaped) are possible when *AB* cavitand **2** is used in the self-assembly reaction; only one is obtained in the case of *AC* cavitand **3**. In addition, the self-assembly of *AB*-dibridged cavitand **2** with dinuclear Pd/Pt metal precursors **5a** and **5b** has been studied. At this level of complexity, the self-assembly can lead to more than one structure. Several different final structures have been envisioned and their formation analyzed in silico and in solution. Out of the three possible cyclic structures (dimer, trimer, and tetramer), only the entropically favored dimer **6a** (**6b**) is formed, as predicted from molecular modeling and demonstrated by PGSE NMR experiments.

Introduction

Metal-directed self-assembly is one of the most useful strategies for the generation of complex molecular architectures.[1] Many concepts have been proposed to predict which species should self-assemble in solution.[2] These considerations are mainly based on the information stored in the building blocks, such as the number of ligands, their relative orientation in space, and the geometry imposed by the selection of a particular metal ion. It appears from the literature that rational design of metallosupramolecular structures is a reliable method.[3] However, an increasing number of examples deviates from the expected structures, like "unexpected" triangle−square equilibration from mixtures of 90° angular units and linear ligands.[4−6] The resulting products usually have similar thermodynamic stability as a result of a balance between entropic and enthalpic factors, and they are in a dynamic equilibrium in solution. The distribution of supramolecular entities in these equilibria can be controlled by the addition of guest molecules as template[7] or by changing

* Corresponding author. Fax: (+39) 0521-905-472.
[†] Dipartimento di Chimica Organica ed Industriale and Unità INSTM, Università di Parma.
[‡] Dipartimento di Chimica Generale ed Inorganica, Chimica Analitica, Chimica Fisica, Università di Parma.
[§] Università di Perugia.

(1) Fujita, M.; Tominaga, M.; Hori, A.; Therrien, B. *Acc. Chem. Res.* **2005**, *38*, 369−378.
(2) (a) Caulder, D. L.; Raymond, K. N. *Acc. Chem. Res.* **1999**, *32*, 975−982. (b) MacGillivray, L. R.; Atwood, J. L. *Angew. Chem., Int. Ed.* **1999**, *38*, 1018−1033. (c) Leininger, S.; Olenyuk, B.; Stang, P. J. *Chem. Rev.* **2000**, *100*, 853−908. (d) Holliday, B. J.; Mirkin, C. A. *Angew. Chem., Int. Ed.* **2001**, *40*, 2022−2043.
(3) (a) Benkstein, K. D.; Hupp, J. T.; Stern, C. L. *Angew. Chem., Int. Ed.* **2000**, *39*, 2891−2893. (b) Woessner, S. M.; Helms, J. B.; Shen, Y.; Sullivan, B. P. *Inorg. Chem.* **1998**, *37*, 5406−5407. (c) Hartmann, I. L.; Berger, S.; Winter, R.; Fiedler, J.; Kaim, W. *Inorg. Chem.* **2000**, *39*, 4977−4980. (d) Takeda, N.; Umemoto, K.; Yamaguchi, K.; Fujita, M. *Nature* **1999**, *398*, 794−796. (e) Olenyuk, B.; Levin, M. D.; Whiteford, J. A.; Shield, J. E.; Stang, P. J. *J. Am. Chem. Soc.* **1999**, *121*, 10434−10435. (f) Olenyuk, B.; Whiteford, J. A.; Fechtenkotter, A.; Stang, P. J. *Nature* **1999**, *398*, 796−799.

10.1021/jo052460m CCC: $33.50 © 2006 American Chemical Society
Published on Web 02/21/2006

SCHEME 1. Synthesis of *AB* and *AC* Bidentate Cavitand Ligands 2 and 3

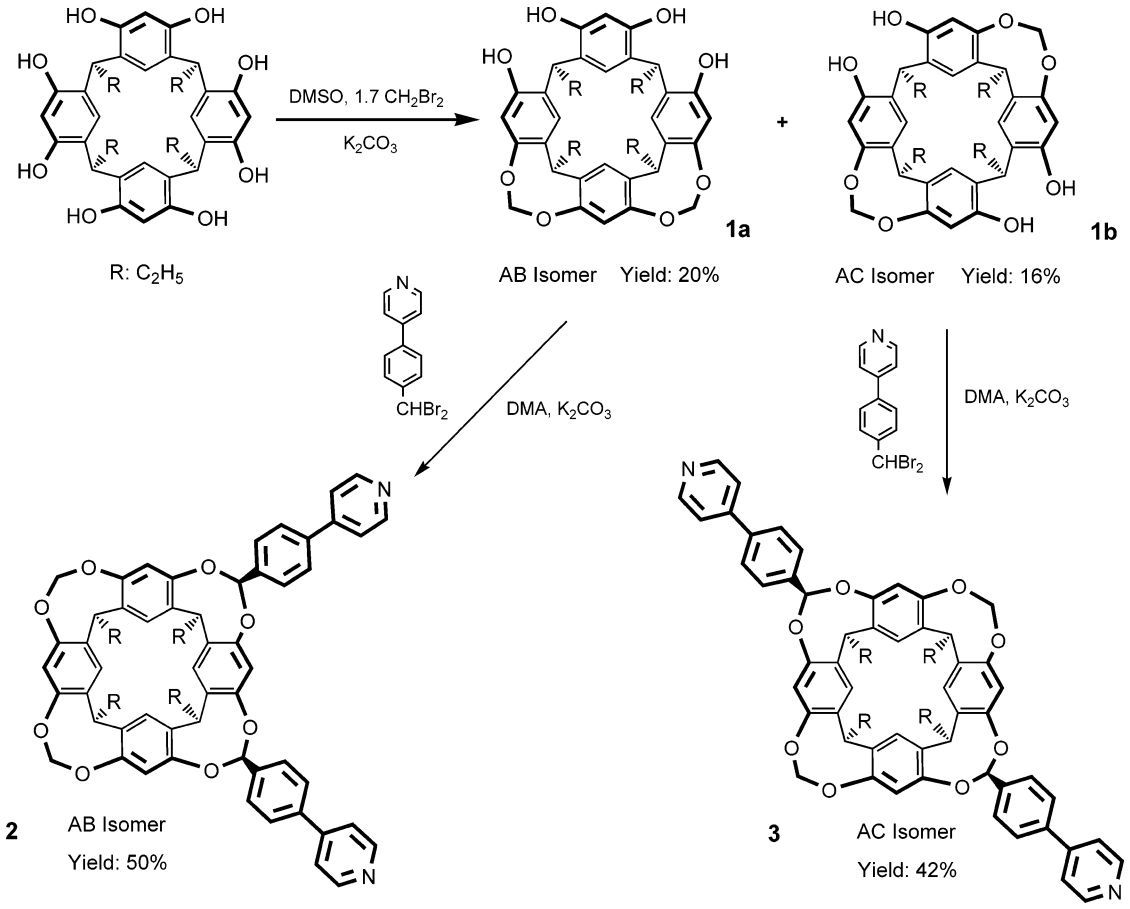

environmental conditions such as concentration, temperature, and pressure.[8] In a previous work, we have studied the self-assembly of monodentate cavitand ligands with mono and dinuclear metal precursors.[9] In this article, we will focus our attention on the metal-directed self-assembly of bidentate cavitand ligands with the same type of metal precursors, aiming at the generation of large cavitand frameworks. For this purpose, dipyridyl-based cavitands have been prepared and their self-assembling options explored. An integrated approach, involving ESI MS characterization, computational calculations, nuclear Overhauser effect (NOE),[10] and pulsed field gradient spin−echo (PGSE)[11] NMR investigations in solution, has been used to characterize the resulting structures.

Results and Discussion

Synthesis of Dibridged Phenylpyridyl Cavitands. To extend the self-assembly protocol toward the generation of large cavitand frameworks, at least two ligand moieties must be introduced at the upper rim of cavitands. For this purpose, we have designed and synthesized bidentate *AB* and *AC* phenylpyridyl-dibridged cavitands (Scheme 1).

The preparation of cavitands **2** and **3** requires first the introduction of two methylene bridges on the starting ethyl-footed resorcinarene. This reaction is performed in dry DMSO using only 1.7 equiv of CH_2Br_2 to minimize the formation of tri- and tetrabridged compounds.[12] Traces of tribridged resorcinarene were obtained. The dibridged resorcinarenes **1a** and **1b** were purified and functionalized with 4-(α,α′-dibromotolyl)-pyridine in dry DMA to give cavitands **2** and **3** (Scheme 1). This type of functionalization at the upper rim of the resor-

(4) (a) Romero, F. M.; Ziessel, R.; Dupont-Gervais, A.; van Dorsselaer, A. *J. Chem. Soc., Chem. Commun.* **1996**, 551−553. (b) Fujita, M.; Sasaki, O.; Mitsuhashi, T.; Fujita, T.; Yazaki, J.; Yamaguchi, K.; Ogura, K. *J. Chem. Soc., Chem. Commun.* **1996**, 1535−1536. (c) Sun, S. S.; Lees, A. J. *J. Am. Chem. Soc.* **2000**, *122*, 8956−8967. (d) Cotton, F. A.; Daniels, L. M.; Lin, C.; Murillo, C. A. *J. Am. Chem. Soc.* **1999**, *121*, 4538−4539. (e) Bark, T.; Duggeli, M.; Stoeckli-Evans, H.; von Zelewsky, A. *Angew. Chem., Int. Ed.* **2001**, *40*, 2848−2851. (f) Cotton; F. A.; Lin, C.; Murillo, C. A. *Acc. Chem Res.* **2001**, *34*, 759−771. (g) Schweiger, M.; Seidel, S. R.; Arif, A. M.; Stang, P. J. *Angew. Chem., Ing. Ed.* **2001**, *40*, 3467−3469. (h) Schweiger, M.; Seidel, S. R.; Arif, A. M.; Stang, P. J. *Inorg. Chem.* **2002**, *41*, 2556−2559. (i) Schalley, C. A.; Muller, T.; Linnartz, P.; Witt, M.; Schafer, M.; Lutzen, A. *Chem.−Eur. J.* **2002**, *8*, 3538−3551.

(5) Sautter, A.; Schmid, D. G.; Jung, G.; Würthner, F. *J. Am. Chem. Soc.* **2001**, *123*, 5424−5430.

(6) Yamamoto, T.; Arif, A. M.; Stang, P. J. *J. Am. Chem. Soc.* **2003**, *125*, 12309−12317.

(7) Ma, G.; Jung Y. S.; Cluing, D. S.; Hong, J.-I. *Tetrahedron Lett.* **1999**, *40*, 531−534.

(8) (a) Fujita, M.; Aoyagi, M.; Ogura, K. *Inorg. Chim. Acta* **1996**, *246*, 53−57. (b) Mamula, O.; Monlien, F. J.; Porquet, A.; Hopfgartner, G.; Merbach, A. E.; von Zelewsky, A. *Chem.−Eur. J.* **2001**, *7*, 533−539.

(9) Menozzi, E.; Busi, M.; Ramingo, R.; Campagnolo, M.; Geremia, S.; Dalcanale, E. *Chem.−Eur. J.* **2005**, *11*, 3136−3148.

(10) Neuhaus, D.; Williamson, M. *The Nuclear Overhauser Effect in Structural and Conformational Analysis*; Wiley-VCH: New York, 2000.

(11) (a) Johnson, C. S., Jr. *Prog. Nucl. Magn. Reson. Spectrosc.* **1999**, *34*, 203. (b) Price, W. S. *Concepts Magn. Reson.* **1997**, *9*, 299. (c) Price, W. S. *Concepts Magn. Res.* **1998**, *10*, 197. (d) Stilbs, P. *Prog. Nucl. Magn. Reson. Spectrosc.* **1987**, *19*, 1. (e) Stejskal, E. O.; Tanner, J. E. *J. Chem. Phys.* **1965**, *42*, 288.

(12) Timmerman, P.; Boerrigter, H.; Verboom, W.; Van Hummel, J. G.; Harkema, S.; Reinhoudt, D. N. *J. Inclusion Phenom.* **1994**, *19*, 167−191.

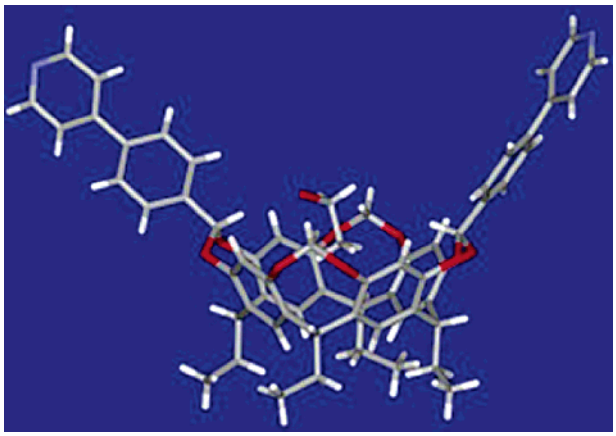

FIGURE 1. X-ray crystal structure of cavitand **3** grown from CH_2Cl_2/EtOH.

cinarene molecules is stereoselective,[13] giving only the *out*−*out* isomers, as proved by ^{1}H NMR analysis. Three different isomers could be formed with different orientations of the phenylpyridyl group, either inward (*i*) or outward (*o*) with respect to the cavity.[14] The formation of the isomers with one or two arms pointing into the cavity is prevented by the bulkiness of the phenylpyridyl group. Therefore, only the desired *out*−*out* isomers were formed in good yields in both cases, with no trace of *in*−*in* and *in*−*out* isomers. Since the metal direct self-assembly requires cavitands with functionalized ligands in a diverging spatial orientation, the *out*−*out* (*AB*, *AC*) isomers have the desired geometry for our purpose. The X-ray crystal structure of the *out*−*out AC* phenylpyridyl cavitand (**3**) was obtained. This crystal structure clearly shows that the two phenylpyridyl groups are oriented outside the cavity in the correct orientation to undergo self-assembly. Inside the cavity there is a molecule of ethanol, the cosolvent used to grow the crystals (Figure 1).

Self-Assembly of *fac*-Br(CO)$_3$Re *AC* Ditopic Complex. Cavitand **3** has been used in the self-assembly of kinetically stable ditopic complexes. [Re(CO)$_5$Br] has been chosen as metal precursor because it is one of the few octahedral complexes that undergoes cis ligand exchange exclusively, due to the remarkable trans effect of carbonyl ligands. Typically, nitrogen ligands replace two equatorial *cis*-CO units of [Re(CO)$_5$Br] to give neutral *fac*-[Re(CO)$_3$L$_2$Br] complexes.[15] Ditopic complex **4** was prepared by refluxing [Re(CO)$_5$Br] with cavitand **3** in a 1:1.2 molar ratio in $CHCl_3$ for 24 h (Scheme 2). A single product was isolated after purification by column chromatography. The ^{1}H NMR spectrum exhibits well-resolved signals for a single highly symmetrical ligand environment with the typical lowfield shift of the pyridyl protons due to metal coordination. The $[M + Na]^+$ ion at $m/z = 2631$ was detected as the molecular ion of complex **4** in the ESI MS spectrum.

The *fac* stereochemistry of complex **4** is confirmed by the FT IR data of the CO stretching region: the three-band pattern at 2030, 1929, and 1890 cm^{-1} is consistent with the facial arrangement of the three CO units in the coordination sphere,[16] and the ^{13}C NMR spectrum exhibits a resonance at 191.9 ppm, typical of an axial CO unit. The same self-assembly procedure conducted on the *AB* bidentate cavitand ligand **2** led to the formation of two complexes (**A**, **B**, see Supporting Information), which have been separated by chromatography. They present almost identical spectroscopic signatures. On the basis of the available spectroscopic data, we suggest that the two ditopic complexes present different arrangements of the cavitand ligands: a C-shaped configuration where the two cavities are facing each other (Clam-shell type configuration)[9] and an S-shaped configuration[17] where the cavities are in a diverging orientation.[18] The interconversion of the two complexes is frozen at room temperature, where the two complexes are kinetically stable. Thus far, all our attempts to assign the correct configuration to the two isomers via X-ray crystallography and PGSE spectroscopy have failed (Supporting Information). The introduction of a second pyridyl ligand on the cavitand skeleton confers conformational rigidity to the corresponding complexes, leading to the desired face-to-face arrangements of the concave sites of the cavitands. On the other side, in the case of *AB* cavitand **2**, this further geometrical constraint leads to the formation of two kinetically stable products. Therefore, only *AC* cavitand **3** is amenable to univocal self-assembly with mononuclear metal precursors.

Self-Assembly of Cavitand-Based Architectures 6a, 6b. The idea of generating microporous materials with embedded molecular recognition elements prompted us to investigate the self-assembly properties of *AB* difunctionalized[19] cavitand **2** as corner units with Pd$_2$(tppb)(CF$_3$SO$_3$)$_4$ (**5a**) and Pt$_2$(tppb)(CF$_3$SO$_3$)$_4$ (**5b**)[9] bimetallic linear spacers (tppb = 1,2,4,5-tetrakis(diphenylphosphino) benzene).[20] Our goal was to obtain a well-defined supramolecular structure by simply mixing the two building blocks in a 2:1 ratio. A unique self-assembled structure can be formed only if it is strongly favored over the others thermodynamically. Our building blocks are compatible with different cyclic assemblies: the possible structures are dimer, trimer, and tetramer (named after the number of bimetallic linear spacers involved; see Scheme 3). ^{1}H NMR analysis showed the disappearance of **2** and the formation of a set of sharp signals compatible with one of the structures indicated, but not with oligomers. ^{1}H NMR experiments at different concentrations and temperatures have been performed to reveal a possible equilibrium between different structures. Decreasing the concentration to 1 mM did not change the ^{1}H NMR spectrum, nor did increasing the temperature to 323 K (Figure 2).

Theoretically high dilution conditions should favor the dimer over the trimer and tetramer.[21] Only multiple charged ions were detected by ESI MS spectrometry, since the molecular ions of all predicted structures are beyond the ESI MS instrument

(13) (a) Xi, H.; Gibb, C. L. D.; Gibb, B. C. *J. Org. Chem.* **1999**, *64*, 9286−9288. (b) Pinalli, R.; Cristini, V.; Sottili, V.; Geremia, S.; Campagnolo, M.; Caneschi, A.; Dalcanale, E. *J. Am. Chem. Soc.* **2004**, *126*, 6516−6517.

(14) (a) Lippmannt, T.; Wilde, H.; Dalcanale, E.; Mavilla, L.; Mann, G.; Heyer, U.; Spera, S. *J. Org. Chem.* **1995**, *60*, 235−242. (b) For a discussion on in−out isomerism, see: Alder, R. W.; East, S. P. *Chem. Rev.* **1996**, *96*, 2097−2112.

(15) (a) Dinolfo, P. H.; Hupp, J. T. *Chem. Mater.* **2001**, *13*, 3113−3125. (b) Lee, S. J.; Lin, W. *J. Am. Chem. Soc.* **2002**, *124*, 4554−4555.

(16) (a) Vitali, D.; Calderazzo, F. *Gazz. Chim. Ital.* **1972**, *102*, 587−596. (b) Giordano, P. J.; Wrighton, M. S. *J. Am. Chem. Soc.* **1979**, *101*, 2888−2897.

(17) (a) Tucci, F. C.; Renslo, A. R.; Rudkevich, D.; Rebek, J., Jr. *Angew. Chem., Int. Ed.* **2000**, *39*, 1076−1079. (b) Cram, P. J.; Tunstad, L. M.; Kruobler, C. B. *J. Org. Chem.* **1982**, *57*, 528−532.

(18) The alternative possibility of diastereoisomeric differentiation due to the relative orientation of Br substituents on the two Re centers can be disregarded by analogy with the case of chiral Re-based molecular squares: Lee, S. J.; Lin, W. *J. Am. Chem. Soc.* **2002**, *124*, 4554−4555.

(19) Under the same self-assembly conditions, the AC isomer **3** leads to polymeric material.

(20) McFarlane, H. C. E.; McFarlane, W. *Polyhedron* **1988**, *7*, 1875−1879.

SCHEME 2. Self-Assembly of *fac*-Br(CO)$_3$Re *AC* Ditopic Complex 4

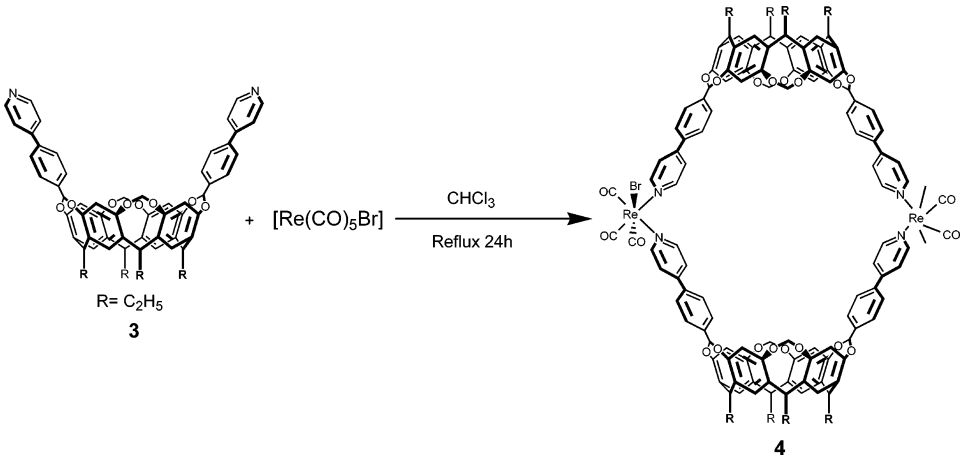

SCHEME 3. Self-Assembly of Nanoporous Structures[a]

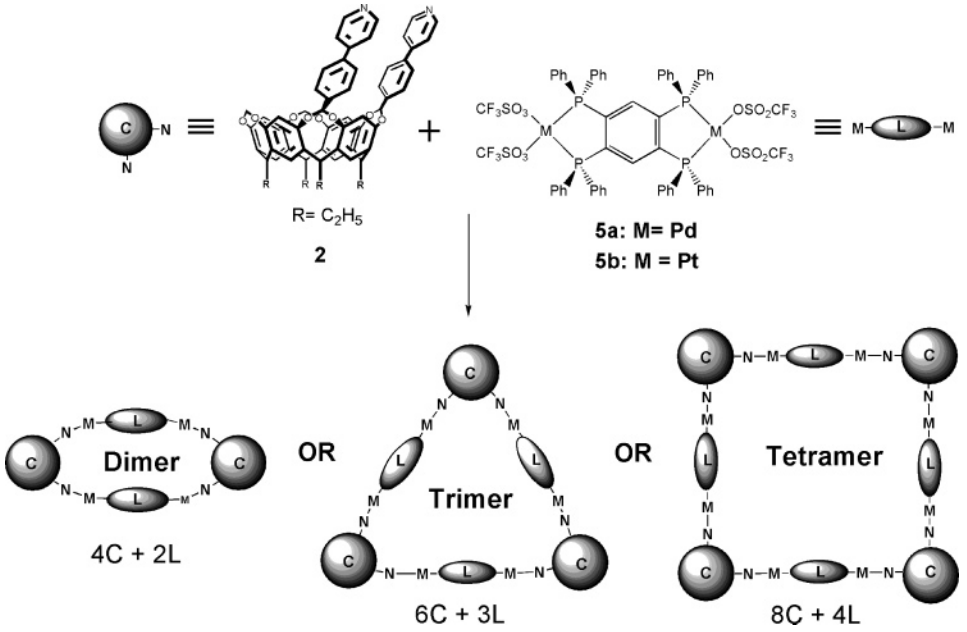

[a] C = ditopic cavitand ligand (**2**). L = dinuclear metal precursor (**5a** or **5b**).

detection limit. All ions detected can be interpreted in terms of both dimer or tetramer, excluding the formation of the trimer (Table 1). It is worth noting that the observed ESI MS ion patterns (Supporting Information) show the expected odd−even sequence of multiple charged ions for the dimer, while for the tetramer they are compatible only with the even ions. The loss of counterions two by two, albeit possible, is unlikely.

Molecular Modeling Studies. Spartan[22] MMFF force field calculations of dimer, trimer, and tetramer were performed with the dual purpose of (i) finding the minimum energy structure for each complex and (ii) evaluating the dimensions of the three objects to support experimental PGSE NMR data. The lowest energy conformer of each structure is shown in Figures 3−5. The semi-axes of the three objects, approximated to ellipsoids, have been calculated from their minimized structures and are reported in the captions of the figures. The formation of the dimeric structure requires a slight bending of the M-tppb-M spacers (Figure 3b). The formation of the cyclic trimeric structure is possible only if four of the six square-planar complexes are turned into distorted tetrahedral complexes (Figure 4), because this is the necessary condition for the closure of the macroring. This ligand geometry cannot be accommodated in the real compound, since both Pd and Pt can form exclusively square-planar complexes. Therefore, the resulting trimeric structure is forbidden with Pd and Pt metal precursors. This prediction is confirmed by mass spectrometric analyses, where the multiple charge ions belonging to the trimer are totally absent.

The simulation of the tetrameric structure is shown in Figure 5. Two of the four M-tppb-M connectors are affected by severe distortion around the phosphorus atoms, while keeping the square-planar coordination of the metal centers. As a consequence, the entire structure is somehow squeezed. Comparison of the relative distortions of the ideal geometries in the dimer and in the tetramer indicates that the former is favored. Since both dimer and tetramer are compatible with ESI MS and NMR measurements and with molecular modeling, PGSE NMR

(21) (a) Chi, X.; Guerin, A. J.; Haycock, R. A.; Hunter, C. A.; Sarson, L. D. *Chem. Commun.* **1995**, 2563−2565. (b) Ercolani, G. *J. Phys. Chem. B* **1998**, *102*, 5699−5703.

(22) *Spartan 04*; Wavefunction, Inc.: Irvine, CA. http://www.wavefun-.com.

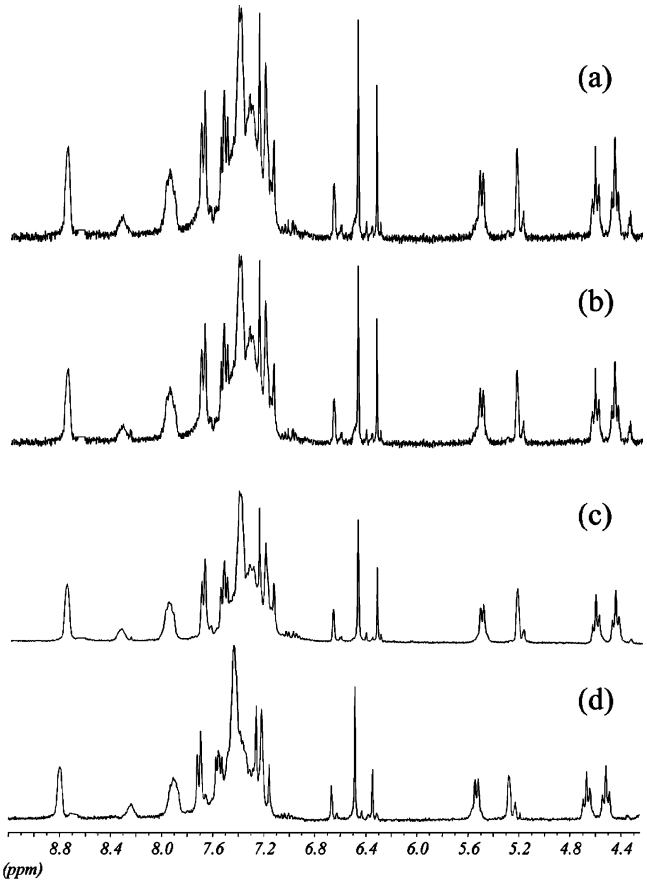

FIGURE 2. Influence of concentration and temperature on self-assembled structure **6a**. ^{1}H NMR (300 MHz, $CDCl_3$). (a) $T = 300$ K, [1.0 mM]. (b) $T = 300$ K, [2.0 mM]. (c) $T = 300$ K, [10.0 mM]. (d) $T = 323$ K, [10.0 mM].

TABLE 1. ESI MS of Self-Assembled Structures 6a and 6b

dimer (*m*/*z*)	**6a** [**2** + **5a**]	**6b** [**2** + **5b**]	tetramer (*m*/*z*)
M^{3+}	2206 (20%)	2325 (5%)	M^{6+}
M^{4+}	1618 (100%)	1706 (10%)	M^{8+}
M^{5+}	1265 (70%)	1335 (30%)	M^{10+}
M^{6+}	1029 (30%)	1088 (100%)	M^{12+}

experiments were undertaken to determine which species were present in solution.

PGSE Measurements. Characterization based on X-ray crystallography is often hampered by difficulties in growing high-quality crystals from assemblies containing large cavities. This was the case for complexes **6a**,**b** that were consequently characterized in solution by mono- and bidimensional NMR methods including ^{1}H PGSE. The latter allows determining the translational self-diffusion coefficient (D_t) and, consequently, estimating the size of diffusing particles in solution.[23,24] In fact, from D_t the average hydrodynamic radius (r_H) of the diffusing particles can be derived taking advantage of the Stokes−Einstein equation [$D_t = kT/(c\pi\eta r_H)$], where k is the Boltzmann constant, T is the temperature, c is a numerical factor that for large molecules as those investigated here can be reasonably placed equal to 6, and η is the solution viscosity. Tetrakis-(trimethylsilyl)silane (TMSS), whose dimension is known from the literature,[25] was used as internal standard. The methodology to obtain accurate r_H values has been described elsewhere.[26]

PGSE NMR measurements were carried out for **6a** in $CDCl_3$ to discriminate between dimer and tetramer predominance. The presence of ^{19}F nuclei on the triflate counterion allowed us to

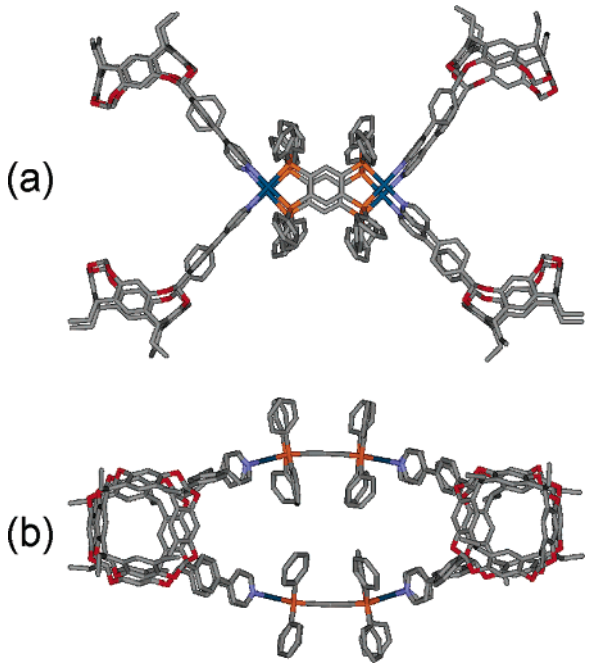

FIGURE 3. Molecular modeling of the cationic part of the dimeric self-assembled structure **6a**. (a) Side view. (b) Top view. Calculated values of the semi-axes: 18.3, 11.8, and 11.7 Å.

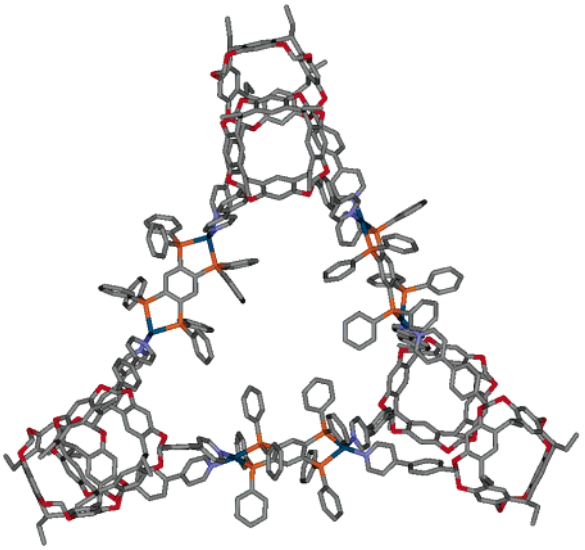

FIGURE 4. Molecular modeling of the cationic part of the hypothetic trimeric self-assembled structure. Calculated values of the semi-axes: 22.8, 18.3, 11.7 Å.

(23) For a review on the application of diffusion measurements in supramolecular chemistry, see: Cohen, Y.; Avram, L.; Frish, L. *Angew. Chem., Int. Ed.* **2005**, *44*, 520−554.

(24) (a) Otto, W. H.; Keefe, M. H.; Splan, K. E.; Hupp, J. T.; Larive, C. K. *Inorg. Chem.* **2002**, *41*, 6172−6174. (b) Zuccaccia, D.; Pirondini, L.; Pinalli, R.; Dalcanale, E.; Macchioni, A. *J. Am. Chem. Soc.* **2005**, *127*, 7025−7032.

(25) Dinnebier, R. E.; Dollase, W. A.; Helluy, X.; Kümmerlen, J.; Sebald, A.; Schmidt, M. U.; Pagola, S.; Stephens, P. W.; van Smaalen, S. *Acta Crystallogr.* **1999**, *B55*, 1014.

(26) Zuccaccia, D.; Macchioni, A. *Organometallics* **2005**, *24*, 3476−3486.

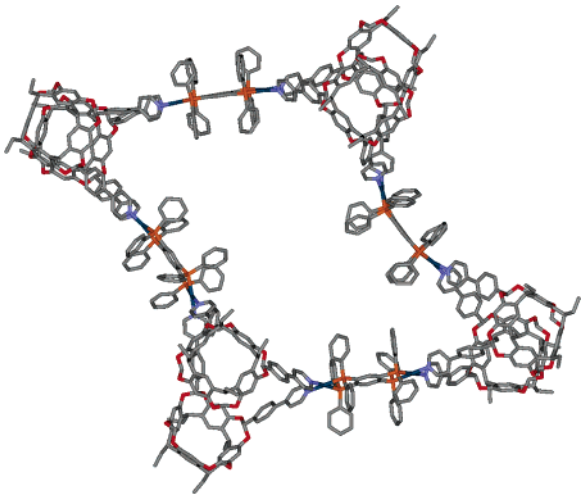

FIGURE 5. Molecular modeling of the cationic part of the hypothetic tetrameric self-assembled structure. Calculated values of the semi-axes: 30.7, 17.8, and 11.7 Å.

TABLE 2. Diffusion Coefficient (D_t) and Hydrodynamic Radius (r_H) of the Species in Solution Obtained via ^{1}H and ^{19}F PGSE NMR Experiments ($CDCl_3$), Compared with the Theoretical Values of the Semi-Axes (*a*, *b*, and *c*) of the Ellipsoid Objects, Describing Cavitand 2 and Dimer 6a, Structures Obtained from the Molecular Modeling (MMFF Force Field Spartan)

	D_t	r_H (Å)	*a* (Å)	*b* (Å)	*c* (Å)
cavitand **2** ^{1}H PGSE	5.1	7.9	6.8	5.9	4.7
6a ^{1}H PGSE	2.4	16.0	18.3	11.8	11.7
6a ^{19}F PGSE	2.5	15.2	18.3	11.8	11.7

perform both ^{1}H and ^{19}F PGSE experiments and, consequently, to independently evaluate the size of the cation and the aggregation level of the anion. The determined r_H for **6a** (16.0 and 15.2 Å from ^{1}H and ^{19}F PGSE experiments, respectively; Table 2) nicely approaches the average value of the semi-axes of the dimeric structure deriving from Spartan calculations assumed to have an ellipsoid shape (Figure 3). On the other hand, r_H of **6a** is much lower than the value expected for the semi-axes for the corresponding ellipsoid of the tetrameric architecture (see Figure 5). On the basis of these experiments, we found that the dimension of the self-assembled complex is consistent with the entropically favored dimeric structure, where only six building blocks are linked together. It is worth noting that the D_t and r_H values derived from ^{1}H and ^{19}F PGSE experiments are very close, indicating that most of the anions translate with the cationic moiety (Table 2).

^{19}F, ^{1}H HOESY NMR experiments were carried out with the aim of understanding if the anions form an intimate adduct and the relative anion−cation orientation(s).[24,27] In the ^{19}F, ^{1}H HOESY NMR spectrum (Figure 6), several interionic NOEs were observed, suggesting that intimate ionic adducts are mainly present in solution. In detail, $CF_3SO_3^-$ showed NOE with Py*H*$_o$, $(PPh_2)_4$Ar*H*, and other aromatic protons of the phosphine and pyridyne rings whose resonances overlap (Figure 6). No interionic NOE contact was observed between $CF_3SO_3^-$ and protons belonging to the cavitand (see, for example, the absence of NOEs between the counterion and the two well-distinguished

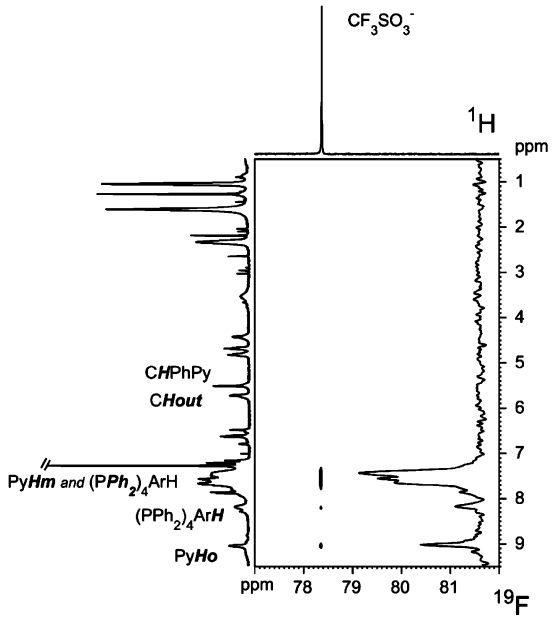

FIGURE 6. ^{19}F, ^{1}H HOESY NMR spectrum (376.65 MHz, 300 K, $CDCl_3$) of complex **6a**.

resonances C*H*PhPy and C*H*$_{out}$ in Figure 6). The counterions are located close to the Pd centers where the positive charge is formally accumulated.

Conclusions

This study has shown that predicting the outcome of self-assembly protocols of bidentate cavitand ligands with mono/ditopic metal precursors is not straightforward. The difficulty arises from the combined effects of the face-to-face (C-shaped isomer) versus face-to-back (S-shaped isomer) positioning of the cavitand ligands in the complexes and the *AB* versus *AC* positioning of the pyridyl ligand groups. The exclusive formation of a single, well-defined molecular structure requires the balancing of the two factors through the appropriate choice of the metal precursors, as shown in the case of ditopic Re-cavitand complex **4** and tetratopic Pd/Pt complexes **6a**,**b**. In the latter case, both entropic and enthalpic factors cooperate to stabilize the dimer over the other species, as predicted by molecular modeling and demonstrated by PGSE NMR.

This work represents a first step toward the generation of a ligands/metal precursors library for the self-assembly of metal organic frameworks[28] featuring embedded molecular recognition sites.

Experimental Section

Ethyl-footed resorcinarene,[29] 4-(α,α′-dibromotolyl)pyridine,[13b] $Pd_2(tppb)(CF_3SO_3)_4$, and $Pt_2(tppb)(CF_3SO_3)_4$[9] were prepared according to literature procedures.

X-ray Analysis. The molecular structure of compound **3** was determined by single-crystal X-ray diffraction methods. Intensity data and cell parameters were recorded at low temperature (173 K) on a CAD diffractometer (Cu Kα radiation). The intensities were

(27) For a review on the application of NOE NMR spectroscopy in the determination of relative anion−cation orientation(s), see: Macchioni, A. *Eur. J. Inorg. Chem.* **2003**, 195−205.

(28) Rowsell, J. L. C.; Yaghi, O. M. *Microporous Mesoporous Mater.* **2004**, *73*, 3−14.

(29) Tunstad, L.; Tucker, J. A.; Dalcanale, E.; Weiser, J.; Bryant, J. A.; Sherman, J. C.; Helgeson, R. C.; Knobler, C. B.; Cram, D. J. *J. Org. Chem.* **1989**, *54*, 1305−1312.

corrected for Lorentz and polarization but not for absorption. The structures were solved by direct methods using the SIR92 program[30] and refined on F_o^2 by full-matrix least-squares procedures, using the SHELXL-97 program.[31] All non-hydrogen atoms were refined with anisotropic atomic displacements.The hydrogen atoms were included in the refinement at idealized geometry (C−H 0.95 Å) and refined "riding" on the corresponding parent atoms. The weighting scheme used in the last cycle of refinement was $w = 1/[\sigma^2F_o^2 + (0.1537P)^2]$ (where $P = (F_o^2 + 2F_c^2)/3$). Molecular geometry calculations were carried out using the PARST97 program.[32] Experimental details for data collection and structure refinement are reported in Table S1 (see Supporting Information). Crystallographic data (excluding structure factors) for the structure reported have been deposited with the Cambridge Crystallographic Data Centre as supplementary publication No. CCDC-284035 and can be obtained free of charge on application to the CCDC, 12 Union Road, Cambridge CB2 1EZ, U.K. Fax: +44-1223/336-033. E-mail: deposit@ccdc.cam.ac.uk.

NOE Measurements. The ^{1}H NOESY[33] NMR experiments were acquired by the standard three-pulse sequence or by the PFG version.[34] Two-dimensional ^{19}F, ^{1}H HOESY NMR experiments were acquired using the standard four-pulse sequence or the modified version.[35] The number of transients and the number of data points were chosen according to the sample concentration and to the desired final digital resolution. Semiquantitative spectra were acquired using a 2-s relaxation delay and 400-ms mixing times.

PGSE Measurements. ^{1}H and ^{19}F PGSE NMR measurements were performed by using the standard stimulated echo pulse sequence on a 400 MHz spectrometer equipped with a GREAT 1/10 gradient unit and a QNP probe with a Z-gradient coil, at 296 K without spinning. The shape of the gradients was rectangular, their duration (δ) was 4−5 ms, and their strength (G) was varied during the experiments. All the spectra were acquired using 32 K points, a spectral width of 5000 (^{1}H) and 18 000 (^{19}F) Hz, and processed with a line broadening of 1.0 (^{1}H) and 1.5 (^{19}F) Hz. The semilogarithmic plots of $\ln(I/I_0)$ versus G^2 were fitted using a standard linear regression algorithm; the R factor was always higher than 0.99. Different values of Δ, "nt" (number of transients), and number of different gradient strengths (G) were used for different samples. The methodology for treating the data has been previously described.[26]

***AB*−*AC* Ethyl-Footed Dimethylene-Bridged Resorcinares (1a, 1b).** A quantity of 1.68 g (12.1 mmol) of K_2CO_3 and 0.20 mL (2.87 mmol) of CH_2Br_2 are added, under nitrogen, to a solution of 1.0 g (1.67 mmol) of resorcinarene (R: C_2H_5) in 30 mL of dry DMSO. The purple mixture is stirred in a sealed tube at 90 °C for 3 h. The reaction is quenched by addition of 10% HCl (aq) solution, and the resulting mixture is extracted with CH_2Cl_2. The organic layer is washed with water (3 × 15 mL), dried over Na_2SO_4, and evaporated. The black crude product obtained is purified in two steps: first by column chromatography (SiO_2, CH_2Cl_2/AcOEt 7:3) to extract the tribridged resorcinarene from the mixture of *AB*−*AC*-dibridged isomers; then a second column chromatography (SiO_2, CH_2Cl_2/EtOH 95:5) on the *AB*−*AC* mixture gives the dibridged *AB* resorcinarene **1a** as white solid in 20% yield (0.21 g) and the *AC* resorcinarene **1b** also as a white solid in 16% yield (0.17 g).

***AB* Isomer (1a):** ^{1}H NMR ($CDCl_3$, 300 MHz) δ 0.91 (t, 6H, J = 7.1 Hz), 1.03 (t, 6H, J = 7.2 Hz), 2.17 (m, 8H), 4.17 (t, 2H, J = 7.1 Hz), 4.42 (d, 2H, J = 7.1 Hz), 4.63 (t, 2H, J = 8.2 Hz), 5.72 (d, 2H, J = 7.1 Hz), 6.32 (s, 2H), 6.37 (s, 1H), 6.49 (s, 1H), 6.96 (s, 1H), 7.19 (s, 2H), 7.26 (s, 1H); MS (CI, *m*/*z*) 625 $(MH)^+$; mp 275−280 °C; R_f (CH_2Cl_2/EtOH, 95:5) = 0.24.

***AC* Isomer (1b):** ^{1}H NMR ($CDCl_3$, 400 MHz) δ 0.91 (t, 6H, J = 7.1 Hz), 1.03 (t, 6H, J = 7.2 Hz), 2.18 (m, 8H), 4.25 (t, 2H, J = 7.1 Hz), 4.39 (d, 2H, J = 7.1 Hz), 4.69 (t, 2H, J = 8.2 Hz), 5.70 (d, 2H, J = 7.1 Hz), 6.31 (s, 4H), 7.18 (s, 4H); MS (CI, *m*/*z*) 625 $(MH)^+$; mp 260−275 °C; R_f (CH_2Cl_2/EtOH, 95:5) = 0.21.

***AB*-Dibridged Tolylpyridyl Cavitands *Out*−*Out* Isomer (2).** A quantity of 0.315 g (0.96 mmol) of 4-(α,α′-dibromotolyl)pyridine and 0.36 g (2.6 mmol) of K_2CO_3 are added under nitrogen to a solution of 0.20 g (0.32 mmol) of **1a** in 15 mL of dry DMA. The mixture is stirred in a sealed tube at 80 °C for 16 h. The reaction is quenched by addition of 10 mL of water, and the resulting mixture is extracted with 15 mL of CH_2Cl_2. The organic layer is washed with water (3 × 15 mL), dried over Na_2SO_4, and evaporated. The brown crude product obtained is purified by column chromatography (SiO_2, hexane/acetone/EtOH 7:2:1) to give compound **2** (*out*−*out* isomer) as a white solid in 50% yield (0.15 g).

^{1}H NMR ($CDCl_3$, 300 MHz) δ 1.02−1.09 (m, 12H), 2.27−2.39 (m, 8H), 4.47 (d, 2H, J = 7.2 Hz), 4.70 (t, 2H, J = 8.1 Hz), 4.86 (t, 2H, J = 8.1 Hz), 5.54 (s, 2H), 5.77 (d, 2H, J = 7.1 Hz), 6.52 (s, 1H), 6.64 (s, 2H), 6.72 (s, 1H), 7.17 (s, 1H), 7.22 (s, 2H), 7.26 (s, 1H), 7.53 [d, (AA′ part of an AA′XX′ system), 4H, J = 8.2 Hz], 7.72 [m, (AA′ part of an AA′XX′ system), 4H, J_o = 6.5 Hz, J_m = 2.0 Hz], 7.83 [m, (XX′ part of an AA′XX′ system), 4H], 8.69 [bs, (XX′ part of an AA′XX′ system), 4H]; MS (CI, *m*/*z*) 956 $(MH)^+$; mp 238−243 °C; R_f (hexane/acetone/EtOH, 7:2:1) = 0.24. Anal. Calcd for $C_{62}H_{54}N_2O_8$: C, 77.97; H, 5.70; N, 2.93. Found: C, 77.82; H, 5.90; N, 2.77.

***AC*-Dibridged Tolylpyridyl Cavitands *Out*−*Out* Isomer (3).** A quantity of 0.3 g (0.92 mmol) of 4-(α,α′-dibromotolyl)pyridine and 0.35 g (2.5 mmol) of K_2CO_3 are added under nitrogen to a solution of 0.19 g (0.31 mmol) of **1b** in 15 mL of dry DMA. The mixture is stirred in a sealed tube at 80 °C for 16 h. The reaction is quenched by addition of 10 mL of water, and the resulting mixture is extracted with 15 mL of CH_2Cl_2. The organic layer is washed with water (3 × 15 mL), dried over Na_2SO_4, and evaporated. The brown crude obtained is purified by column chromatography (SiO_2, hexane/acetone/EtOH 7:2:1) to give compound **3** (*out*−*out* isomer)-as a white solid in 42% yield (0.12 g).

^{1}H NMR ($CDCl_3$, 300 MHz) δ 1.02−1.08 (m, 12H), 2.30−2.36 (m, 8H), 4.49 (d, 2H, J = 7.2 Hz), 4.71 (t, 2H, J = 8.1 Hz), 4.82 (t, 2H, J = 8.1 Hz), 5.50 (s, 2H), 5.76 (d, 2H, J = 7.2 Hz), 6.64 (s, 4H), 7.21 (s, 4H), 7.51 [d, (AA′ part of an AA′XX′ system), 4H, J = 8.2 Hz], 7.70 [m, (AA′ part of an AA′XX′ system), 4H], 7.80 [m, (XX′ part of an AA′XX′ system), 4H], 8.66 [bs, (XX′ part of an AA′XX′ system), 4H]; MS (CI, *m*/*z*) 956 $(MH)^+$; mp 245−250 °C; R_f (hexane/acetone/EtOH 7:2:1) = 0.30. Anal. Calcd for $C_{62}H_{54}N_2O_8$: C, 77.97; H, 5.70; N, 2.93. Found: C, 77.76; H, 5.92; N, 2.75.

***fac*-Br(CO)$_3$Re *AC* Ditopic Cavitand Complex (4).** A quantity of 41.0 mg (4.29×10^{-2} mmol) of cavitand **3** is added to a solution of 14.0 mg (3.43×10^{-2} mmol) of [$Re(CO)_5Br$] in $CHCl_3$ and heated at reflux for 24 h. After solvent evaporation, the product is purified by column chromatography (SiO_2, $CHCl_3$/AcOEt 6:4) to give the *fac*-ditopic cavitand complex **6** in 40% yield (30.0 mg).

^{1}H NMR ($CDCl_3$, 300 MHz, T 323 K) δ 1.05 (m, 24H), 2.27−2.36 (m, 16H), 4.46 (d, 4H, J = 6.7 Hz), 4.73 (t, 4H, J = 7.9 Hz), 4.83 (t, 4H, J = 7.8 Hz), 5.47 (s, 4H), 5.74 (d, 4H, J = 6.7 Hz), 6.60 (s, 8H), 7.24 (s, 8H), 7.54 (d, (AA′ part of an AA′XX′ system), 8H, J = 6.2 Hz), 7.69 (d, (AA′ part of an AA′XX′ system), 8H, J = 8.1 Hz), 7.82 [d, (XX′ part of an AA′XX′ system), 8H, J = 8.1 Hz], 8.93 [d, (XX′ part of an AA′XX′ system), 8H, J = 6.2 Hz]; ^{13}C NMR ($CDCl_3$, 75 MHz) δ 12.2 (CH_3), 29.3 (CH_2), 30.9 (CH_2), 38.2 (CH), 99.5 (OCH_2O), 106.8 (CHPhPy), 116.4 (CH), 120.8 (CH), 123.3 (CH), 127.2 (CH), 127.4 (CH), 136.6 (Cq), 138.3 (Cq), 138.9 (Cq), 140.7 (Cq), 149.9 (Cq), 153.8 (CH), 154.6 (CH), 191.9 (CO_{ax}), 195 (CO_{eq}); FT IR (KBr) ν_{CO} = 2030, 1929, 1890 cm^{-1};

(30) Altomare, A.; Cascarano, G.; Giacovazzo, C.; Gualiardi, A.; Burla, M. C.; Polidori, G.; Camalli, M. *J. Appl. Crystallogr*. **1994**, *27*, 435−436.
(31) Sheldrick, G. M. *SHELX-97, Program for Crystal Structure Refinement*; University of Göttingen: Göttingen, Germany, 1997.
(32) Nardelli, M. *J. Appl. Crystallogr*. **1995**, *28*, 659.
(33) Jeener, J.; Meier, B. H.; Bachmann, P.; Ernst, R. R. *J. Chem. Phys.* **1979**, *71*, 4546.
(34) Wagner, R.; Berger, S. *J. Magn. Reson. A* **1996**, *123*, 119.
(35) Lix, B.; Sönnichsen, F. D.; Sykes, B. D. *J. Magn. Reson. A* **1996**, *121*, 83.

MS (ESI, *m*/*z*, (%)) calcd for $C_{130}H_{108}N_4O_{22}Re_2Br_2$ (M) 2610.52, $(M - CO + H)^+$ 2583.52, found 2585 (50), $(M + Na)^+$ 2633.51, found 2630 (100). Anal. Calcd for $C_{130}H_{108}N_4O_{22}Re_2Br_2$: C, 59.81; H, 4.17; N, 2.15. Found: C, 59.65; H, 4.39; N, 2.07.

General Procedure for the Self-Assembly of Frameworks 6a,b. The compounds are assembled by simply mixing cavitand **3** with metal precursors $Pd_2(tppb)(CF_3SO_3)_4$ (**5a**) and $Pt(tppb)(CF_3SO_3)_4$ (**5b**) in a 2:1 molar ratio at room temperature.

6a: ^{1}H NMR ($CDCl_3$, 300 MHz) δ 0.85 (m, 48H), 2.19−2.23 (m, 32H), 4.15 (bd, 8H), 4.47 (t, 8H, J = 8.1 Hz), 4.62 (t, 8H, J = 7.8 Hz), 5.23 (bs, 8H), 5.51 (bd, 8H), 6.33 (s, 4H), 6.42 (bs, 8H), 6.67 (bs, 4H), 7.15 (s, 4H), 7.21 (s, 8H), 7.30−7.68 (m, 100H), 7.70 [d, (AA′ part of an AA′XX′ system), 16H, J = 8.2 Hz], 7.96 [bd, (XX′ part of an AA′XX′ system), 16H], 8.34 (bd, 4H), 8.77 [bd, (XX′ part of an AA′XX′ system), 16H]; ^{1}H NMR ($CDCl_3$, 300 MHz, 323 K) δ 0.85 (m, 48H), 2.19−2.23 (m, 32H), 4.19 (bd, 8H), 4.51 (t, 8H, J = 8.0 Hz), 4.62 (t, 8H, J = 7.5 Hz), 5.28 (bs, 8H), 5.53 (d, 8H, J = 7.8 Hz), 6.34 (s, 4H), 6.48 (bs, 8H), 6.67 (bs, 4H), 7.15 (s, 4H), 7.21 (s, 8H), 7.27−7.57 (m, 100H), 7.70 [d, (AA′ part of an AA′XX′ system), 16H, J = 8.0 Hz], 7.91 [bd, (XX′ part of an AA′XX′ system), 16H], 8.24 (bd, 4H), 8.79 [bd, (XX′ part of an AA′XX′ system), 16H]; MS (ESI, *m*/*z*, (%)) calcd for $C_{364}H_{300}N_8O_{56}Pd_4P_8S_8F_{24}$ (M) 7061.2, $(M - 3CF_3SO_3)^{3+}$ 2204.8, found 2206 (20), $(M\text{-}4CF_3SO_3)^{4+}$ 1616.4, found 1618 (100), $(M - 5CF_3SO_3)^{5+}$ 1263.3, found 1265 (70), $(M - 6CF_3SO_3)^{6+}$ 1027.9, found 1029 (30).

6b: ^{1}H NMR ($CDCl_3$, 300 MHz) δ 0.89 (m, 48H), 2.20−2.25 (m, 32H), 4.29 (bs, 8H), 4.54 (t, 8H, J = 8.0 Hz), 4.69 (t, 8H, J = 7.7 Hz), 5.26 (s, 8H), 5.58 (d, 8H, J = 7.3 Hz), 6.44 (s, 4H), 6.53 (bs, 8H), 6.66 (bs, 4H), 7.14 (s, 4H), 7.20 (s, 8H), 7.30−7.70 (m, 100H), 7.72 [d, (AA′ part of an AA′XX′ system), 16H, J = 8.2 Hz], 8.10 [bd, (XX′ part of an AA′XX′ system), 16H], 8.35 (bd, 4H), 8.82 [bd, (XX′ part of an AA′XX′ system), 16H]; MS (ESI, *m*/*z*, (%)) calcd for $C_{364}H_{300}N_8O_{56}Pt_4P_8S_8F_{24}$ (M) 7417.5, $(M - 3CF_3SO_3)^{3+}$ 2323.5, found 2325 (5), $(M\text{-}4CF_3SO_3)^{4+}$ 1705.4, found 1706 (10), $(M\text{-}5CF_3SO_3)^{5+}$ 1334.5, found 1335 (30), $(M\text{-}6CF_3SO_3)^{6+}$ 1087.3, found 1088 (100).

Acknowledgment. This work was supported by MURST (FIRB-Nanoorganization of Materials with Magnetic and Optical Properties COFIN 2003-Proprietà di singole molecole ed architetture molecolari funzionali supportate, and COFIN 2004-Nuove strategie per il controllo delle reazioni: interazione di frammenti molecolari con siti metallici in specie non convenzionali). The instrumental facilities at the Centro Interfacoltà di Misure G. Casnati of the University of Parma were used. We also thank Dr. G. Guglielmetti of the Istituto G. Donegani, Novara, for the ESI MS analyses of the Re complexes.

Supporting Information Available: Synthesis, molecular modeling, and PGSE data of ditopic complexes **A** and **B**. Molecular modeling of cavitand **2**. X-ray crystallographic data of cavitand **3**. ^{1}H NMR table of compounds **6a** and **6b**, scheme of molecular dimer orientation of **6a** and **6b**, and ESI MS spectra of self-assembled architecture **6b**. This material is available free of charge via the Internet at http://pubs.acs.org.

JO052460M